Changes to the water balance over a century of urban development in two neighborhoods: Vancouver, Canada

AGU100 ADVANCING EARTH AND SPACE SCIENCE

Water Resources Research

RESEARCH ARTICLE
10.1029/2017WR022445

Key Points:
- Long-term (1920-2010) changes in contrasting suburban water balances are examined
- Irrigation found to be the most important factor in determining water and energy balances
- Urbanization caused an increasing trend of up to 4 mm/year in runoff

Supporting Information:
- Supporting Information S1

Correspondence to:
T. V. Kokkonen,
tom.kokkonen@helsinki.fi

Citation:
Kokkonen, T. V., Grimmond, C. S. B., Christen, A., Oke, T. R., & Järvi, L. (2018). Changes to the water balance over a century of urban development in two neighborhoods: Vancouver, Canada. *Water Resources Research*, *54*, 6625–6642. https://doi.org/10.1029/2017WR022445

Received 20 DEC 2017
Accepted 19 AUG 2018
Accepted article online 27 AUG 2018
Published online 19 SEP 2018

Changes to the Water Balance Over a Century of Urban Development in Two Neighborhoods: Vancouver, Canada

T. V. Kokkonen[1], C. S. B. Grimmond[2], A. Christen[3], T. R. Oke[4], and L. Järvi[1,5]

[1]Institute for Atmospheric and Earth System Research/Physics, Faculty of Science, University of Helsinki, Helsinki, Finland, [2]Department of Meteorology, University of Reading, Reading, UK, [3]Environmental Meteorology, Faculty of Environment and Natural Resources, University of Freiburg, Freiburg im Breisgau, Germany, [4]Department of Geography, University of British Columbia, Vancouver, British Columbia, Canada, [5]Helsinki Institute of Sustainability Science, University of Helsinki, Helsinki, Finland

Abstract Hydrological cycles of two suburban neighborhoods in Vancouver, BC, during initial urban development and subsequent urban densification (1920–2010) are examined using the Surface Urban Energy and Water Balance Scheme. The two neighborhoods have different surface characteristics (as determined from aerial photographs) which impact the hydrological processes. Unlike previous studies of the effect of urbanization on the local hydrology, densification of already built lots is explored with a focus on the neighborhood scale. Human behavioral changes to irrigation are accounted for in the simulations. Irrigation is the dominant factor, accounting for up to 56% of the water input on an annual basis in the study areas. This may surpass garden needs and go to runoff. Irrigating once a week would provide sufficient water for the garden. Without irrigation, evaporation would have decreased over the 91 years at a rate of up to 1.4 mm/year and runoff increased at 4.0 mm/year with the increase in impervious cover. Similarly without irrigation, the ratio of sensible heat flux to the available energy would have increased over the 91 years at a rate of up to 0.003 per year. Urbanization and densification cause an increase in runoff and increase risk of surface flooding. Small daily runoff events with short return periods have increased over the century, whereas the occurrence of heavy daily runoff events (return period > 52 days) are not affected. The results can help us to understand the dominant factors in the suburban hydrological cycle and can inform urban planning.

1. Introduction

Urban hydrological processes directly affect the safety and comfort of citizens as well as infrastructure, and thus, the ability to analyze and predict hydrological behavior in cities is critical. Sustainable urban planning and infrastructure design require realistic hydrological predictions but are limited by the complexity of urban hydrological systems due to tightly coupled relationships between human and natural systems in urban areas (House-Peters & Chang, 2011). Here knowledge of historical effects of urbanization on hydrological processes can play an informative role.

Urban development within a catchment causes drastic changes in land cover and has major effects on the urban climate and hydrological cycle. In general, urbanization is considered the most dominant factor altering the hydrology of an area (e.g., Leopold, 1968) by changing water use, increasing surface runoff, and decreasing infiltration and evaporation causing increased probability of flooding (e.g., Rodriguez et al., 2003). The primary impact comes from the increase in the fraction of paved surfaces. As runoff volume is governed to a large extent by infiltration capacity of the surface, the area that rainfall can infiltrate is greatly reduced due to increased impervious areas (e.g., roads, pathways, buildings, and parking). Thus, their accurate representation in urban hydrological models is critical (Ramamurthy & Bou-Zeid, 2014; Tokarczyk et al., 2015) despite many impervious surfaces not being 100% impermeable. A secondary effect of urbanization on the water balance is the loss of vegetation reducing evaporation and increasing surface runoff further. Third, garden irrigation can have a substantial effect on the urban hydrological cycle particularly in areas where many gardens are present (Best & Grimmond, 2016; Demuzere et al., 2014; Mitchell et al., 2001, 2003; Oke et al., 2017). Grimmond and Oke (1986a) found that for a suburban watershed lawn, irrigation increased annual

evaporation comparable to a rural watershed in the same region. Given the substantial volumes of water used for garden irrigation, it can also cause great stress to water resources during periods of drought. Thus, many cities have imposed irrigation restrictions or total bans when there is water scarcity to lower the risk of reservoir levels being depleted too quickly (e.g., Gober et al., 2010; Hall & Schreier, 1996; Kennedy et al., 2004).

After initial urbanization, areas typically undergo subsequent densification of impervious cover caused by building extensions and garages, addition of laneway houses, expansion of driveways, and so forth. Thus, urban densification affects the hydrological cycle in a similar way to the initial urbanization process (e.g., Dams et al., 2013; Pauleit et al., 2005). However, the impact of densification on urban hydrology has yet to be analyzed with highly detailed data on all the variables and parameters affecting an area. Past studies on the effect of urban densification on the hydrology have focused on new neighborhoods, blocks, or unbuilt lots between built areas (i.e., initial urbanization; e.g., Dams et al., 2013; Egeinbrod et al., 2011; Pauleit et al., 2005), but the impact originating from densification of existing urban structure remains to date unstudied. Many studies of long-term hydrological effects of urbanization mostly focus on large (continental, country, or city) spatial scales or lack the detailed characteristics of the area of interest (Fletcher et al., 2013; Sailor, 2011). Additionally, the impact of garden irrigation restrictions on local hydrological cycle has not been studied in detail as most previous studies focused on short-term effects on the hydrological conditions (e.g., Demuzere et al., 2014) or effects on the energy balance (i.e., cooling effect; e.g., Gober et al., 2009).

To investigate long-term densification, detailed surface cover changes at the scale of individual buildings are needed. Commonly, land cover fractions are determined from aerial photographs (e.g., Goldshleger et al., 2009; Pauleit et al., 2005; White & Greer, 2006), but these may not be available with sufficient frequency to determine the changes in area that have taken place, or the quality of historical aerial photographs might be unsuitable for detailed land cover determination. Even the latest automated algorithms for surface cover classification with manually annotated training cannot determine surface cover fractions from aerial photographs in sufficient detail to capture incremental changes in densification (Tokarczyk et al., 2015). However, manual analysis can capture the densification occurring in late decades. Census data can provide population densities change.

The objective of this paper is to examine the hydrological changes of two urban neighborhoods in Vancouver, BC, between 1920, before the initial urbanization occurred, and 2010 when replacement second and third generations of larger detached houses with secondary units (laneway houses) have occurred. The effect of initial urbanization and subsequent densification determined from aerial photographs on local hydrological conditions are analyzed. Realistic irrigation patterns based on local surveys with water use restrictions imposed in Vancouver area varying from free irrigation to total ban are implemented and their effect on the water balance examined. The reanalysis WATCH forcing data (Weedon et al., 2011, 2014) are used as the meteorological forcing for urban land surface model SUEWS (Järvi et al., 2011; Ward, Kotthaus, et al., 2016).

2. Methods

2.1. Study Sites

The two suburban areas (Oakridge and Sunset neighborhoods) are approximately 3 km apart on fairly flat terrain in the southeastern part of Vancouver, BC, Canada (Table 1). Both residential areas are characterized by 1–2-storey-detached houses (LCZ 6, Stewart & Oke, 2012) but have different land cover fractions and lot sizes. The more prosperous (e.g., Canada Statistics, 1988) Oakridge neighborhood has bigger lots and houses and well-maintained gardens with more automatic irrigation than in Sunset. In 2010, 24% of Oakridge was covered with buildings, 29% paved surfaces, 14% with trees and shrubs, and 32% grass of which 61% was automatically irrigated and population density was 26 inhabitants per hectare. The Sunset site is more densely built with 29% of buildings, 37% of paved surfaces, 7% trees and shrubs, and 27% grass with only 1% of automatic irrigation systems and population density of 82 inhabitants per hectare (see section 2.3.2). The study sites exact water monitoring areas are described in detail in Christen et al. (2009) and have been the focus of past work on the urban energy and water balance (Cleugh & Oke, 1986; Grimmond, 1992; Grimmond & Oke, 1986a, 1986b, 1991, 1999a; Järvi et al., 2011; Kalanda et al., 1980; Kokkonen et al., 2018; Oke, 1979; Oke & McCaughey, 1983, 1989, 2017; Schmid et al., 1991).

Vancouver experiences a maritime temperate climate (Oke & Hay, 1994). The winter time precipitation is approximately four times greater than summer precipitation, and therefore, there is substantial amount of garden irrigation in summer (Grimmond & Oke, 1986a). For the last century, the climate of Vancouver has been

Table 1
Properties of the Study Areas Assumed Constant Throughout the Study Period 1920–2010

Study site	Oakridge	Sunset
Location of the study area	49.225° N, 123.133° E	49.224° N, 123.084° E
Total area (ha)	22.5	14.9
Altitude asl (m)	85	82

Note. Irrigation period is from 1 May to 31 August. Calculation of z_{0m} and z_{dm} (m) used mean building and tree height (Grimmond & Oke, 1999b). Modeling height aboveground level is 28 m. z_{0m} = aerodynamic roughness length; z_{dm} = zero displacement height; asl = above sea level.

influenced by the climate change, and a significant positive trend in both annual precipitation and mean annual temperature has been observed (Ministry of Environment, 2016; see also Figure 1).

2.2. Model Description

Version V2016a of the Surface Urban Energy and Water Balance Scheme (SUEWS; Ward, Järvi, et al., 2016; Ward, Kotthaus, et al., 2016) is used for the long-term hydrological modeling. In the model, the simulated area (neighborhood or catchment scale) is separated into paved, buildings, evergreen trees/shrubs, deciduous trees/shrubs, grass, bare soil, and water surface types, and dynamic interaction between these is allowed. Below each surface type, except water, there is a single soil layer.

The water balance is

$$P + I_e = E + R + \Delta S, \tag{1}$$

where P is precipitation, I_e is irrigation, E is evapotranspiration, R is runoff, and ΔS is the net change in surface and soil water storage. Precipitation is a model input, whereas the other components are simulated. Irrigation is parametrized based on the daily mean air temperature (T_d) and days since rain (t_r; Järvi et al., 2011):

$$I_e = f_{irr}[f_{aut}(b_{0,a} + b_{1,a}T_d + b_{2,a}t_r) + (1 - f_{aut})(b_{0,m} + b_{1,m}T_d + b_{2,m}t_r)], \tag{2}$$

where f_{aut} is the fraction of irrigated area (f_{irr}) using automatic irrigation systems, and $b_{0,a} - b_{2,a}$ and $b_{0,m} - b_{2,m}$ are site specific constants for automatic and manual irrigation, respectively (supporting information Table S4). From observations in Oakridge and Sunset neighborhoods in 2009, $b_{0,m} - b_{2,m}$ is 0.30 times the automatic irrigation coefficients (Järvi et al., 2011). Separate f_{irr} are set for evergreen, deciduous, and grass vegetation types. The irrigation submodel allows further inclusion of different irrigation scenarios allowing specified proportion of houses to irrigate on specific days and times. The daily totals are applied at the hours specified in the user profiles based on day types (e.g., weekday/weekend)

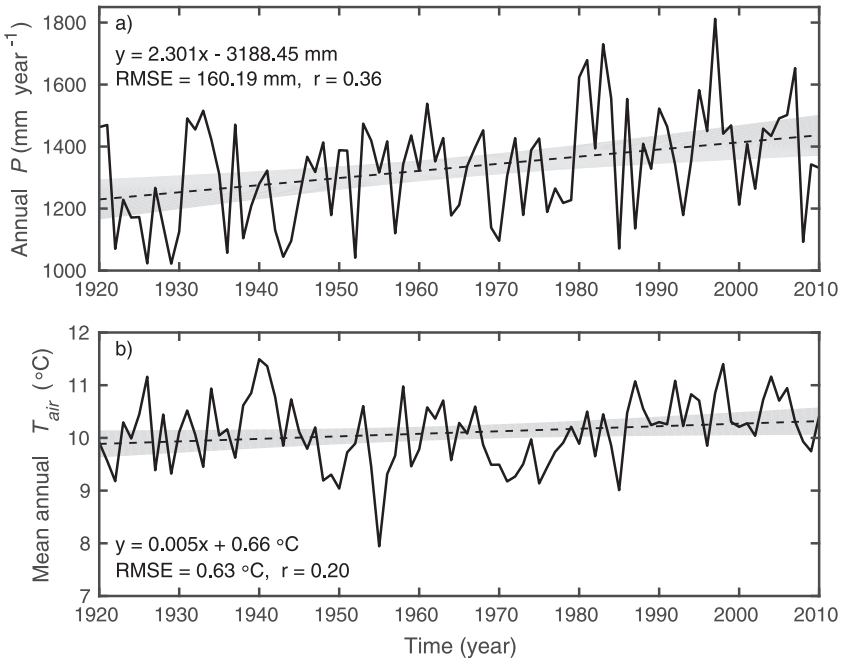

Figure 1. The (a) annual precipitation (P) and (b) mean annual air temperature (T_{air}) from WATCH reanalysis data for Vancouver for the period 1920–2010. The gray areas are nonsimultaneous functional bounds with 95% confidence level. Both study sites use WATCH data from the same grid cell, which is downscaled for the study sites (see section 2.3.1). See section 2.5 for statistics explanation. RMSE = root mean square error.

The evaporation is calculated using the Penman-Monteith equation (Monteith, 1965; Penman, 1948) modified for urban environments (Grimmond & Oke, 1991):

$$Q_E = \frac{s(Q^* + Q_F - \Delta Q_S) + c_p \rho V / r_a}{s + \gamma(1 + r_s/r_a)}, \tag{3}$$

where Q_E is the latent heat flux ($Q_E = L_v E$; L_v is the latent heat of vaporization), Q^* is the net all-wave radiation, Q_F is the anthropogenic heat emission, ΔQ_S is the net storage heat flux, s is the slope of the saturation vapor pressure curve, c_p is the specific heat capacity, ρ is the density of air, V is the vapor pressure deficit of air, γ is the psychometric 'constant', and r_a and r_s are aerodynamic and surface resistances, respectively. In SUEWS, r_s responds to vegetation type (i) through leaf area index and its cover fraction normalized maximum conductance as well as the environmental variables of incoming solar radiation, specific humidity deficit, air temperature, and soil moisture deficit ($\Delta\theta$; Järvi et al., 2011). For the effect of $\Delta\theta$ to surface conductance (g), we use form

$$g(\Delta\theta) = 1 - \exp(G_6(\Delta\theta - (S_1/G_6) + S_2)), \tag{4}$$

where G_6, S_1, and S_2 are parameters related to the maximum $\Delta\theta$ (Table S4). Equation (3) is applicable to dry surfaces. When the surface is completely wet, the surface resistance is set to zero. To link the dry and wet surface stages, r_s is replaced with a redefined surface resistance (Shuttleworth, 1978).

The water storage state for each surface type (i) is calculated with the aid of a running water balance at each time step (Grimmond & Oke, 1991):

$$C_i = C_{i,t-1} + (P_i + I_{e,i} + R_{S2S,i}) - (D_i + E_i), \tag{5}$$

where $C_{i,t-1}$ is the surface storage at previous time step, R_{S2S} is the water flowing from other surfaces (defined based on surface connectivity by the user for the area), and D_i is drainage. Thus, the surface can become wet from precipitation, irrigation, or from hydrologically connected surfaces within the grid. Drainage is calculated from (Falk & Niemczynowicz, 1979):

$$D_i = D_{0,i}(C_{i,t-1})^b. \tag{6}$$

The values used for the maximum drainage rates ($D_{0,i}$) and empirical coefficient (b) are given in Table S3.

The drainage from impervious to pervious surfaces is controlled by the user-defined parameters for the hydrologically connected surfaces based on knowledge of the study area. In our simulations, 6% of water from roofs flows to paved surfaces and 1% to evergreen vegetation, 1% to deciduous vegetation, and 1% to grass. From impervious surfaces, rest of the the drainage goes to surface runoff: first to pipe network and if the pipe capacity is exceeded, flooding at the surface will occur. Currently, water cannot infiltrate to soil directly from impervious surfaces (i.e., cracks are not assumed to exist). The remaining drainage from pervious surfaces infiltrates into the underlying soil increasing the amount of water of each soil store ($C_{\mathrm{soil},i}$). Soil infiltration rate is assumed to be larger than drainage (Grimmond & Oke, 1986b) when hourly rainfall intensities are below 10 mm. If $C_{\mathrm{soil},i}$ exceeds its maximum storage capacity, the water will first attempt to go to the pipe network, and if full, flooding will occur. The total R is the sum of pipe runoff and weighted mean of aboveground runoff of impervious and vegetated surfaces.

If the state of ith surface (C_i) is dry and evaporation occurs, water is removed from soil under pervious surfaces:

$$C_{\mathrm{soil},i} = C_{\mathrm{soil},i,t-1} + R_{I,i} - E_i - R_{BG,i2j} - R_{DS}, \tag{7}$$

where $R_{I,i}$ is the infiltration into subsurface i, R_{DS} is the runoff to deep soil, and $R_{BG,i2j}$ is the belowground horizontal transfer of water between surface types i and j calculated according to (Hillel, 1971):

$$R_{BG,i2j} = -K_{m,i2j}\frac{\Delta H_{i2j}}{X_{i2j}}, \tag{8}$$

where X_{i2j} is the distance between the two stores, ΔH_{i2j} is the pressure head difference of the stores i and j, and $K_{m,i2j}$ is the hydraulic conductivity.

If at this point, a belowground soil storage ($C_{\mathrm{soil},i}$) exceeds its maximum capacity, the water is removed to deep soil as runoff (R_{DS}). After these steps, the area-wide energy and water fluxes and storage changes are

calculated for an individual time step as a weighted function of the extent of the component surface types in the simulated area.

SUEWS has submodels for net all-wave radiation, storage, and anthropogenic heat fluxes. The model uses a 5-min time step during which the surface energy balance components, the surface and soil water states and movements between the surface and soil storages, and surface runoff are calculated (Järvi et al., 2011, 2014).

SUEWS is designed to run using commonly available meteorological variables (wind speed, relative humidity, air temperature, pressure, precipitation, and incoming solar radiation), and in addition, information about the surface characteristics of the modeled area, including plan area fractions, tree and building heights, population density, and human activity profiles, are needed.

2.3. Input Data

The detailed input data required to run SUEWS gathered from various sources for the analyzed period 1920–2010 are described in the following sections. The meteorological forcing data are taken from reanalysis data, whereas historical surface characteristics are from aerial photographs of the study areas, census data, technical reports (Christen et al., 2009; Crawford et al., 2010; Liss et al., 2010; van der Laan et al., 2012), cartographic material, and local surveys. These historical data are available only for certain years, and the missing data are linearly interpolated between the known values to obtain annually changing realistic input data to run SUEWS.

2.3.1. WATCH Forcing Data

The meteorological forcing data are obtained from the WATCH Forcing Data (1919–1979; Weedon et al., 2011) and WATCH Forcing Data-ERA-Interim (1980–2010; Weedon et al., 2014). These data sets have been derived for hydrological modeling purposes from ERA-40 (Uppala et al., 2005) and ERA-Interim (Dee et al., 2011) reanalysis products via sequential interpolation to half-degree resolution with 3- to 6-hr temporal resolution. For the precipitation, we use the Global Precipitation Climatology Centre's GPCCv4/v5/v6 (Schneider et al., 2013) bias correction.

In order to use the WATCH data to provide realistic forcing for local hydrological modeling, a few corrections are needed (Kokkonen et al., 2018). First, the 3- and 6-hr data are linearly interpolated to 1-hr resolution, which is the recommended time resolution of the forcing data for SUEWS V2016a. The precipitation for previous 3 hr is distributed evenly to each hour assuming the precipitation rate is constant for the period. This is considered to be a reasonable assumption as most precipitation is from frontal rain in winter, and the focus of this study is on the long-term water balance. Later releases of SUEWS provide a disaggregation scheme that should be more realistic for precipitation (Ward et al., 2017). Second, the air temperature and pressure are adjusted to the simulation height using environmental lapse rate ($\Gamma = -6.5$ K/km) and the hypsometric equation (Weedon et al., 2010). Third, in order to remove the bias between the WATCH precipitation representing 0.5° horizontal grid and the local city precipitation rates, the reanalysis precipitation is corrected using bias correction with quantile mapping at daily temporal resolution. Assuming the within-day temporal variation of precipitation to be captured by the WATCH forcing data and hourly precipitation intensities to have similar biases within a day. Using these corrections, the WATCH reanalysis data have shown to give reasonable SUEWS model performance at the studied sites in Vancouver (Kokkonen et al., 2018). Due to the corrections needed to the WATCH data, additional periods outside the actual modeling period are needed to avoid interpolation errors and missing data at the beginning and at the end of the time series. In this study, periods of 1 month before and after the modeled period (1919–2010) are used.

2.3.2. Site Characteristics

The detailed surface cover fractions (trees [f_{trees}], grass [f_{grass}], buildings [f_{bldgs}], and paved [f_{paved}]) and number of houses (No_{houses}) needed to estimate the population densities are determined manually from historical aerial photographs (Figure 2 and Table S1) in order to have sufficient detail to capture densification. Photographs are available for 1930, 1938 (Oakridge only), 1946, 1949, 1954, 1959 (poor quality, number of houses only), 1963, 1969, 1979, 1989, 1999, and 2009 (Table S1; City of Vancouver, 2015; Geographic Information Centre, 2015). Only the primary residential buildings are counted, whereas for the surface cover fractions, all the buildings, including garages, are included. The ratio of evergreen and deciduous vegetation needed by SUEWS cannot be determined from the photographs used, so it is assumed to be the same as estimated in 2009 (Liss et al., 2010; 77% of deciduous) for the whole study period.

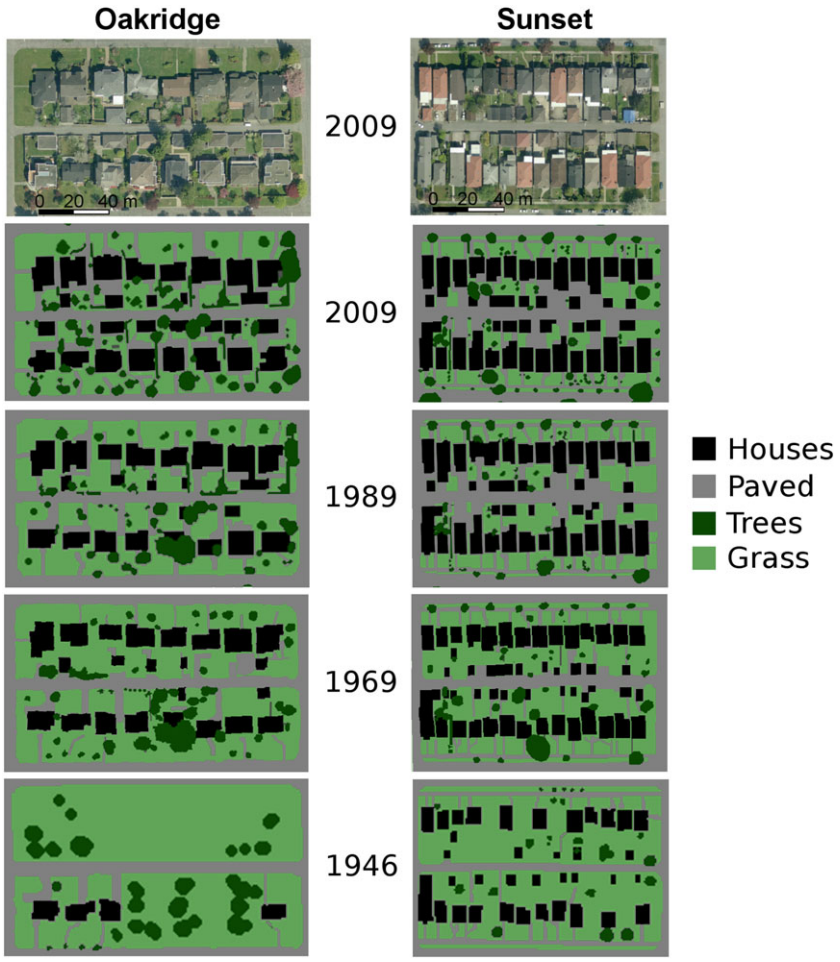

Figure 2. Examples of surface cover fractions determined manually from aerial photographs for Oakridge and Sunset neighborhoods for one example block of the study areas (upper panels) for different years.

Both study areas were initially forested and then clear cut for agriculture before the study period. Afterward, the two sites have developed quite differently (Figure 3 and Table S1). In the Sunset neighborhood, some buildings were already present in the 1920s, and the number of houses gradually increased until 1999. Although the Oakridge neighborhood did not start to develop until the 1940s, all the current built lots were developed by the mid-1950s. While the number of buildings have remained the same, there has been a significant densification of the existing lots post-1979 as the old houses have been progressively replaced with new larger houses and larger garages, terraces, and driveways have been built and expanded. Prior to 1979, the number of houses was steady for many decades, but the fraction of impervious surfaces ($f_{imp} = f_{bldgs} + f_{paved}$) increases (Figure 3). Expansion of driveways during the late decades is seen also at the Sunset neighborhood (Figure 2).

The mean heights of buildings and trees and population density needed are indirectly estimated. The mean building heights in Sunset neighborhood are known for individual houses built before 1965, between 1965–1990 and post-1990 (van der Laan et al., 2012). The mean heights for the whole simulated areas are obtained by using information on the percentage of houses built in certain years available in the census data (1986, 1996, 2001, 2006, and 2011; Canada Statistics, 1988, 1999, 2002, 2012), and the final heights are calculated as a weighted mean from the known heights of individual houses and their proportion in different eras (Text S1). Similarly, the mean tree heights are only known for certain years (1982 and 2009 for Oakridge neighborhood, Grimmond & Oke, 1986a; Liss et al., 2010, and 1987 and 2009 for Sunset neighborhood, Grimmond & Oke, 1991; Liss et al., 2010; Figure 3 and Table S1) and for other years, realistic tree height values are indirectly derived using urban tree growth models described in McPherson et al. (2016a) with empirical equations from McPherson et al. (2016b; see Text S3).

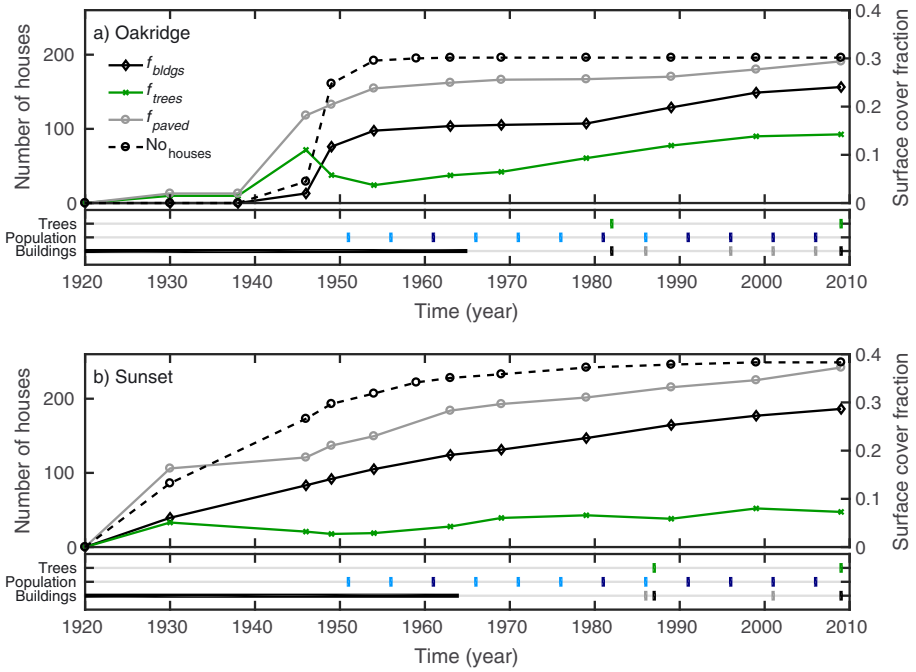

Figure 3. Variation of annual surface cover fractions and number of houses for (a) Oakridge and (b) Sunset neighborhoods for the period 1920–2010. Years with aerial photographs (symbols) are linearly interpolated between (lines). Lower panels are timelines where the markings indicate the individual years when observed data on tree heights (Trees), population densities (Population), and building heights (Buildings) are available. For population density, enumeration area (dark blue) and census tract area (light blue) data are used. For building height, timeline actual measured values (or known values for every year until 1964; black) and when the ratio of the ages of buildings are known (gray; see text for details).

Population densities are determined from census data for either enumeration and dissemination areas that are approximately the size of the study areas or for the much larger census tract areas (Table S1). The population density data are available for 1951, 1956, 1961, 1966, 1971, 1976, 1981, 1986, 1996, 2001, 2006, and 2011 (Dominion Bureau of Statistics, 1953, 1957, 1968; Statistics Canada, 1974, 1978, 1984, 1988, 1999, 2002, 2007, 2012; Vancouver (BC), Planning department, 1963).

2.3.3. Irrigation

Irrigation can be an important water balance component in suburban areas, and thus, its correct description is particularly important. From the modeling perspective, this includes the amount of water used for irrigation, the area irrigated, and possible water use restrictions. The irrigation model (section 2.2) coefficients are determined from observations and surveys in the Oakridge (1982 and 2009) and Sunset neighborhoods (1987 and 2009; Christen et al., 2009; Grimmond & Oke, 1986a, 1991). The available data cover water use, the fraction of

Table 2
Irrigation Restrictions Applied Between 1920 and 2010

Year	Irrigation restrictions
1951–1991	No irrigation restrictions
1992	Total ban for 10 weeks (25 June to 2 September)
1993–2002	Stage 1 restrictions
2003	Stage 1 restriction increased to stage 2 on 5 August. Total ban from 22 August to 30 September
2004 –2010	Stage 1 restrictions

Note. Stage 1 = irrigation is allowed between 4 and 9 a.m. and between 7 and 10 p.m. (1 June to 30 September) on Wednesday and Saturday for even numbered addresses and Thursday and Sunday for odd numbered addresses. Stage 2 = irrigation allowed on 1 day/week: Wednesday for even numbered and Thursday for odd numbered houses (Metro Vancouver, 2010, 2011).

Table 3
Description of Different Model Runs and the Compilation of Input Data Used

Run name	IR	CF	MC
Base run	R	R	R
No restrictions	NoR	R	R
No irrigation	No	R	R
Stage 1	S1	R	R
Stage 2	S2	R	R
Constant surface	NoR	F2010	R

Note. IR = irrigation; CF = cover fractions; MC = meteorological conditions; R = realistic; NoR = no irrigation restrictions; No = no irrigation; S1 = stage 1 irrigation restrictions (see Table 2); S2 = stage 2 irrigation restrictions (see Table 2); F2010 = constant cover fractions from 2010.

irrigated areas, and automatic irrigation systems (Table S2). For other years, required model parameters are derived from historical research.

Initiation of lawn irrigation by sprinkler systems followed the first company (The Rain Bird Corporation) patenting in 1947 the hose end sprinkler for lawns (Rain Bird Corporation, 2016) and 1951 a sales branch opening in Vancouver. Given this, irrigation is assumed to start in 1951. Both study areas were mostly built by the time. The fraction of irrigated lawns is assumed to increase linearly from 1951 till the known values. As the Rain Bird Corporation (2016) patented the first automatic irrigation system designed for residential use in 1968, the automatic irrigation is assumed to start a few years later than the patent (1972). Again, the fractions are linearly interpolated to the known values at both sites.

From surveys and measurements made in Oakridge neighborhood in 1982 (Grimmond & Oke, 1986a) and Sunset neighborhood in 1987 (Grimmond & Oke, 1991), irrigation is allowed to occur between 1 May and 31 August in the model runs. This period is held constant, but weather conditions modify the actual days of irrigation. Since 1992, water use restrictions have been implemented in Vancouver during dry summers. These are accounted for in the simulations (Table 2).

2.4. Experimental Setup

SUEWS is run continuously for the period 1919–2010. Spin-up for 1 year leaves 1920–2010 for analysis. Site characteristics vary (section 2.3), with 1919 assigned the same surface cover information as 1920. Table 1 summarizes the site characteristics remaining constant throughout the modeled period. Model parameters are given in Tables S1–S4. The model is run using interpolated and corrected 1-hr data (Kokkonen et al., 2018; see section 2.3.1) and within the model linearly interpolated to the 5-min time step used. The assumption of equal subhourly rainfall intensity is removed in V2017a of SUEWS with more realistic disaggregation method (Ward et al., 2017).

Multiple model runs with different combinations of input data are performed to capture the effect of different factors on the hydrological components (e.g., effects of irrigation, urbanization, and densification; Table 3). The base run is considered to be the closest to the real conditions with actual surface cover characteristics and irrigation with actual restrictions (Table 2). Additional runs are performed (Table 3): without irrigation, with irrigation without the restrictions (i.e., free irrigation), with stages 1 and 2 irrigation restrictions, and with constant surface cover from 2010 with free irrigation. The latter is to examine the effect of irrigation alone on evaporation and runoff generation.

2.5. Statistical Analysis

The linear least-square correlations among different model variables are analyzed using common statistical tools, including root mean square error (RMSE) and Pearson's correlation coefficient (r). The uncertainties of linear least-square fits ($a = bx + c$) are taken into account by nonsimultaneous functional bounds with 95% confidence level. The long-term changes of daily runoff events are evaluated using occurrence frequency analysis where the return period is calculated using the empirical Weibull (1939) formula, a method recommended by World Meteorological Organization (2011) for hydrological return period analysis. The long-term trend analyses are made with nonparametric Mann-Kendall trend test (Kendall, 1975; Mann, 1945), which does not require the data to be normally distributed and is insensitive to outliers. It is one of the most widely used tests to detect significant trends in hydrological time series (e.g., Hirsch et al., 1982; Lins & Slack, 1999; Pechlivanidis et al., 2017; Zhang et al., 2000) which are often skewed and might contain outliers.

3. Results

3.1. Model Evaluation and Sensitivity

Extensive examinations of SUEWS performance and its sensitivity to different input variables and parametrizations have been made in the past. Good model performances against eddy covariance measured sensible and latent heat fluxes, soil moisture, and surface wetness have been found in Vancouver and Swindon and London (UK; Järvi et al., 2011; Ward, Kotthaus, et al., 2016) and heat fluxes and surface runoff in Helsinki (Järvi et al., 2014, 2017; Karsisto et al., 2016). Other evaluated sites by means of turbulent heat fluxes are located in Dublin,

Hamburg, Melbourne, Phoenix, and Singapore (Alexander et al., 2015, 2016; Demuzere et al., 2017). In addition, Järvi et al. (2011) analyzed the impact of measured versus modeled net all-wave radiation, soil moisture deficit, and irrigation and different parameters of roughness length for heat and surface conductance on Q_E at the Sunset site. SUEWS was found to be the most sensitive to the surface conductance parameters, while using the measured net all-wave radiation, soil moisture deficit and irrigation instead the modeled ones had only minor impact on the model performance. The impact of temporal resolution of forcing precipitation to E and R has been evaluated in Swindon (Ward et al., 2017), where coarser-resolution (3 hr) precipitation was found to overestimate the annual E by 6.6% and underestimate the annual R by 4.1% when compared to the finer-temporal resolution (5 min) forcing data. The largest impacts are seen on days with greatest daily rainfall. Also, impact of infiltration rate was studied (Ward et al., 2017), where ±50% variation of infiltration caused bias up to 3% and 2% in E and R, respectively. Similarly, the sensitivity of SUEWS to WATCH reanalysis forcing data has been evaluated in Vancouver (Kokkonen et al., 2018) showing SUEWS to be the most sensitive to precipitation and incoming solar radiation. Similar results of SUEWS sensitivity to input variables have been found in other studies (Alexander et al., 2015; Ward & Grimmond, 2017).

Here additional sensitivity analysis against selected model parameters impacting particularly the hydrological cycle and model evaluation is made at both studied sites. SUEWS is shown to be more sensitive to soil store capacity (biases of <18% in E and <4% in R) than the soil depth (biases of <4% in E and <1% in R) when the values are changed by ±30% (Figure S1). The values of soil store capacity and soil depth used for the long-term runs (150 and 349 mm, respectively) are based on observations made in Oakridge and Sunset neighborhoods (Grimmond & Oke, 1986a; Hare & Thomas, 1979), therefore represent the best estimate.

SUEWS is relatively independent (bias <2% in E and R) of the value of the drainage parameters used in equation (6) (Figure S3). Using the selected model parameters (Table S3), SUEWS simulates well soil moisture deficit when compared to observations at both sites in 2009 (Figure S2).

In order to estimate the model uncertainty originating from the division of 3-hr precipitation data equally to 5-min time steps, the number of 5-min periods with observed precipitation within each 3-hr precipitation period is calculated for the Sunset site in 2009. On average, 11.9 five-min periods within 3-hr precipitation events have rain which is almost double the number of periods in London (6.0; Ward et al., 2017). Thus, the uncertainties originating from the coarse-resolution precipitation data in Vancouver will most likely be less than the 6.6% in E and 4.1% in R in London. Furthermore, this small bias in annual values can be assumed to be similar between the years and thus should not affect the results.

The indirect methods used to obtain the mean building and tree heights and population densities introduce some uncertainty in the model runs. However, sensitivity tests for Oakridge neighborhood in 2009 (changed ±30%) show SUEWS to be relatively independent of these three site characteristics (Figure S4). Population density has the greatest impact causing deviations of 0.7% on evaporation and 0.1% on runoff.

3.2. Long-Term Changes in the Water Balance Components

The main water inputs to the urban system are precipitation (P) and irrigation (I_e) which are partitioned into evapotranspiration (hereafter evaporation, E) and surface runoff (R) after changes in water storage. Over the analyzed period 1920–2010, both P and I_e have changed with the first having an annual increase of 2.4 mm/year (Figure 1). The effect of these changes together with urbanization is examined relative to the long-term behavior of E and R (Figure 4).

In the base run, with the most realistic model input, E varies between 324–835 and 322–711 mm/year for the Oakridge and Sunset neighborhoods, respectively, and R between 569–2,782 and 605–1,719 mm/year (Figures 4a and 4c). The start of irrigation in 1951 results in an increase in E at both sites (Figure 4a). Its effect on R is smoother, with maximum values reached in 1990 (Figure 4c). From the start of irrigation, the amount of water increases gradually. This is partitioned to E initially until the maximum potential of E is reached, only after that does the additional water starts to run off. Even though I_e occurs only between 1 May and 31 August, it is a major component in the hydrological cycle at both sites. It accounts for 4–56% and 2–38% of annual totals of water input and 29–89% and 21–80% during the irrigation period in Oakridge and Sunset neighborhoods, respectively. E and R are substantially higher in the more prosperous Oakridge than Sunset neighborhood. After the irrigation starts, there is greater area of irrigated lawns and more automatic irrigation systems (Table S2). Irrigation restrictions have reduced E and R at both sites, starting in 1992.

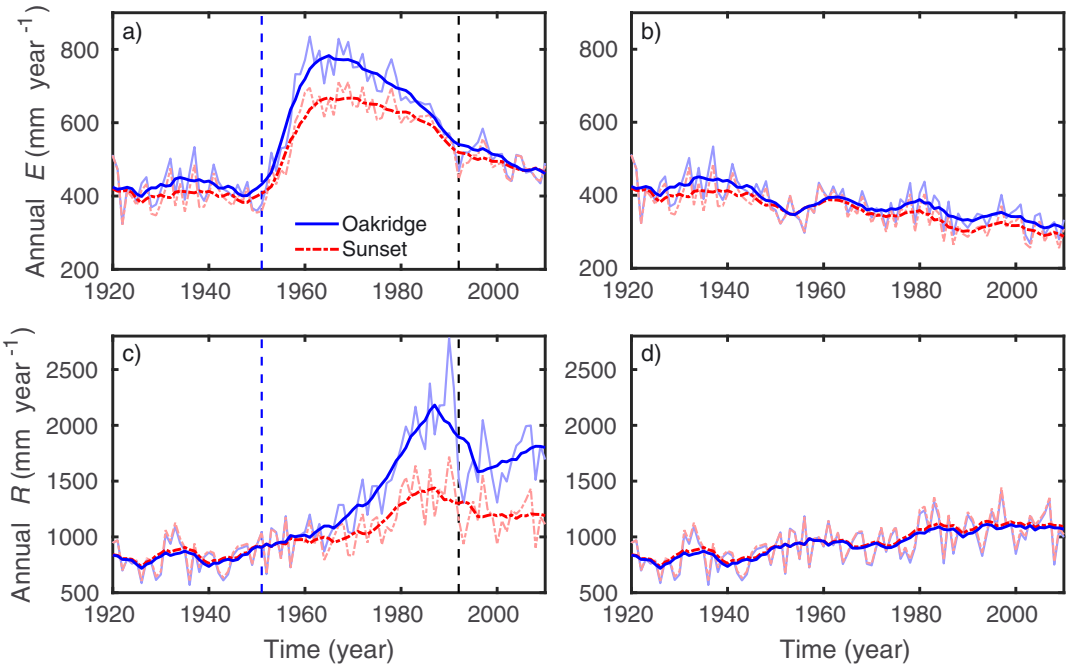

Figure 4. Annual (lighter curves) and 10-year running mean (bold curves). (a, b) Evaporation (*E*) and (c, d) runoff (*R*) for the (a, c) base run and (b, d) no irrigation run over the study period. Start of the irrigation period (1951, blue vertical-dashed line) and start of irrigation restrictions (1992, black vertical-dashed line).

As the strong influence of I_e on both *E* and *R* masks the other effects of urbanization and densification, the no irrigation run is examined (Figures 4b and 4d). A clear decreasing trend (p value $\ll 0.01$) in *E* (1.3 and 1.4 mm/year, average 1920–2010) and increasing trend (p value $\ll 0.01$) in *R* (3.9 and 4.0 mm/year, 1920–2010) are seen in Oakridge and Sunset neighborhoods, respectively. Despite the relative high annual variation, the long-term changes of *E* and *R* are relatively linear and similar between the two study areas even though the urbanization scenarios of the areas are substantially different (Figure 3). The decrease in *E* and increase in *R* in the 1950s are due to a cold period (see Figure 1) decreasing *E* and respectively leading to greater surface runoff. In general, the positive trend seen in air temperature over the study period (Figure 1) has insignificant effect on *E* and *R* as linear correlation analysis gives insignificant correlation between the air temperature and evaporation or runoff (significance level $\alpha = 0.05$).

The irrigation dominates also the partitioning of energy to sensible heat flux (Figure 5a). Irrigation increases evaporation (or latent heat flux) at the expense of the sensible heat flux. There is a clear decrease in Q_H ratio after the irrigation starts in 1951. After *E* (and latent heat flux) reaches its maximum potential (see also Figure 9, section 3.4), urbanization increases Q_H similarly as before the start of the irrigation. Without the irrigation (no irrigation run, Figure 5b), the two study sites have relatively linear and similar long-term changes similarly to the long-term changes of *E* and *R* (Figures 4a and 4c). A clear increasing trend (p value $\ll 0.01$) in Q_H ratio (0.002 and 0.003 per year, average 1920–2010) occurs in Oakridge and Sunset neighborhoods, respectively. However, the higher degree of urbanization in Sunset is evident with a slightly larger proportion of Q_H. The cold period in 1950s resulted in higher proportions of Q_H (Figure 5b) similarly to *R* (Figure 4d) due to decreased amount of evaporation (Figure 4b). The 10-week irrigation ban in 1992 has a visibly higher peak in the Q_H ratio (Figure 5a). Part of the increase in Q_H is related to the increase in anthropogenic heat flux (Q_F) associated with the population density. Q_F reaches around 35 and 10 W/m^2 in Sunset and Oakridge (Figure S5). Changes in Q_F mainly impacts Q_H rather than the water balance.

As the water balance is affected by *P*, to isolate the effects of urbanization and densification, the annual *E* and *R* are normalized by annual *P* and plotted against the impervious surface cover fraction for the no irrigation run (Figure 6). The normalized *R* (i.e., runoff coefficient) is typically used to evaluate the level of urbanization and human influence on local hydrology and partitioning of water to evaporation and runoff (e.g., Barron et al., 2013; Velpuri & Senay, 2013). An increase of 0.1 in the impervious surface cover fraction increases the runoff

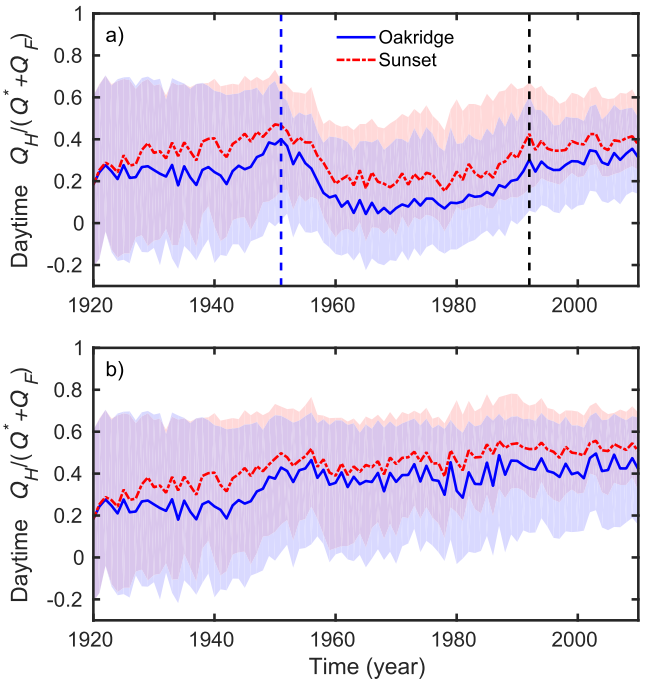

Figure 5. Sensible heat flux ratio for the (a) base run and (b) no irrigation run over the study period showing medians of daytime values and 25th to 75th percentiles (shaded areas). Start of the irrigation period (1951, blue vertical-dashed line) and start of irrigation restrictions (1992, dashed vertical black line).

coefficient by 5% and 4% in Oakridge and Sunset neighborhoods, respectively, and decreases the normalized evaporation by 9% and 7%. The effect of increasing impervious surfaces on both water balance components is quite similar at both study areas. The change in normalized E and R is slightly greater in Oakridge than in Sunset neighborhood, but the difference between the sites is approximately within the error margins of the linear fits (functional boundaries with 95% confidence level). Also, in the Oakridge neighborhood, there are less data for lower impervious fractions due to the more rapid urbanization process. When realistic irrigation is included, the runoff coefficient (i.e., $R/(P+I_e)$) calculated from the yearly totals of base run varies from the minimum values in 1955 (0.53) and 1969 (0.54; f_{imp}: 39% and 50%) to maximum values in 1990 (0.83) and 2007 (0.75; f_{imp}: 47% and 65%) in Oakridge and Sunset, respectively.

Although these runoff coefficients are high compared other residential areas (e.g., Shuster et al., 2005), there is high dependence on precipitation amount, as precipitation fills the soil water storages so that pervious surfaces start to induce runoff (e.g., Boyd et al., 1993; Burton & Pitt, 2002). Vancouver experiences approximately 1,000 mm/year with winter precipitation four times greater than in summer months (Oke & Hay, 1994). Therefore, with the soil storage rather full (Figure S2) during the winter, it is responsible for the high runoff coefficients. These values are in line with previous studies from Vancouver (e.g., Grimmond & Oke, 1986a; Hare & Thomas, 1979).

The dependence of annual runoff coefficients on the annual precipitation is examined at both sites in three decade long development periods to understand how the coefficients have changed (Figure 7): early stage of urbanization (1921–1930; $f_{imp}^{Oakridge} = 0.02$; $f_{imp}^{Sunset} = 0.02–0.22$), middle (1961–1970; $f_{imp}^{Oakridge} = 0.40–0.42$; $f_{imp}^{Sunset} = 0.46–0.50$), and mature (2001–2010; $f_{imp}^{Oakridge} = 0.51–0.53$; $f_{imp}^{Sunset} = 0.63–0.66$).

Over each decade, there is a clear increase in the runoff coefficients (i.e., more runoff produced from precipitation) with increasing amounts of P. This dependence is enhanced with the degree of urbanization (i.e., steeper slopes with time; Figure 7). This indicates that probability of flash floods increases throughout the study period. The differences between the fit lines for 1921–1930 and 1961–1970 (change in mean runoff coefficient: 0.07 and 0.06 in Oakridge and Sunset neighborhoods, respectively) are due to the initial urbanization, but the differences between the fit lines for 1961–1970 and 2001–2010 (change in mean runoff coefficient: 0.07 in both study areas) are due to the densification since there is no initial urbanization occurring between

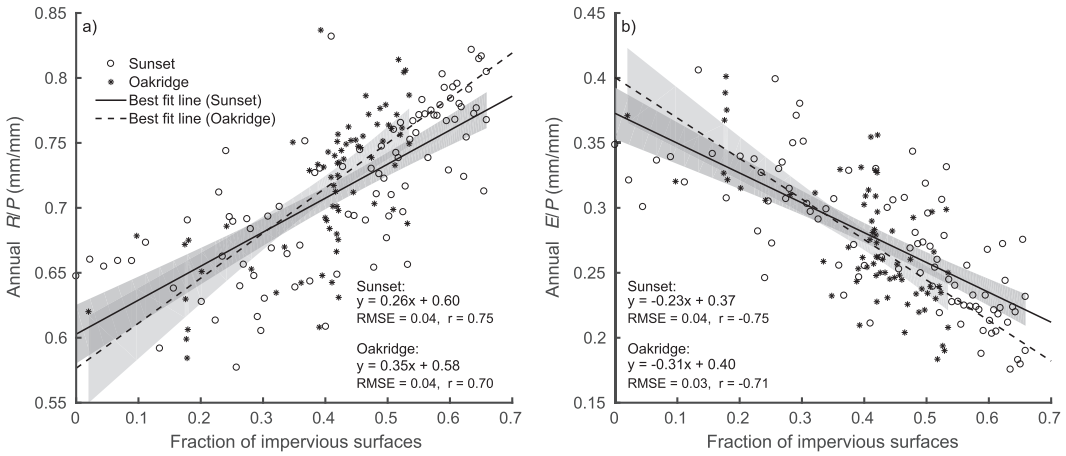

Figure 6. Annual (a) runoff (R) and (b) evaporation (E) normalized with precipitation (P) as a function of fraction of impervious surfaces for the no irrigation run in 1920–2010. The gray areas are nonsimultaneous functional bounds with 95% confidence level. See section 2.5 for statistics explanation.

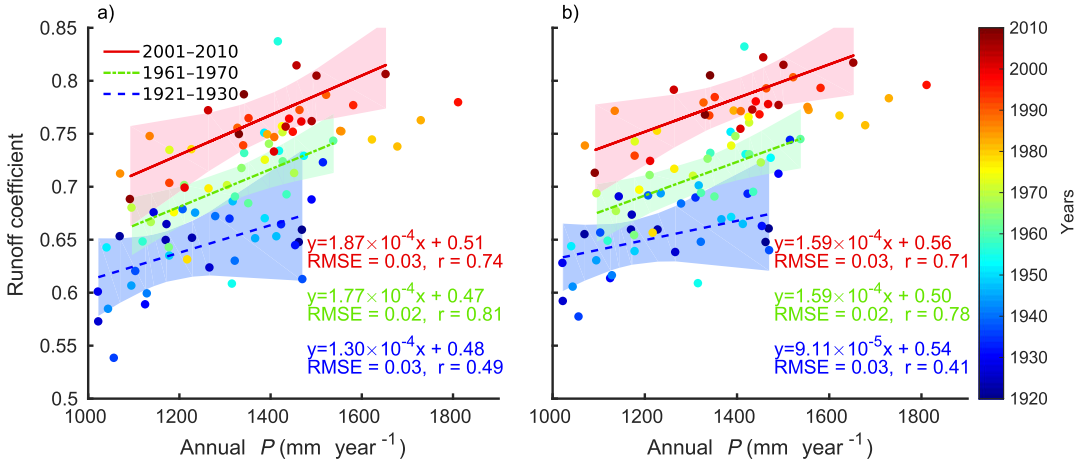

Figure 7. Annual runoff coefficients (colored dots) as a function of precipitation (*P*) for the no irrigation run in (a) Oakridge and (b) Sunset neighborhoods in three development periods: 1921–1930 (early), 1961–1970 (middle), and 2001–2010 (mature). The shaded areas are nonsimultaneous functional bounds with 95% confidence level. See section 2.5 for statistics explanation.

those periods. This substantial increase in impervious surfaces affects the runoff coefficient significantly, and the effect of densification on runoff coefficient is evident for both of the study areas.

3.3. Return Period

In addition to the long-term changes in the water balance components, it is important, particularly from the point of view of sustainable urban planning, to understand how the occurrence of daily runoff events are changing through time. The occurrence frequency analysis shows how a given amount of daily runoff events occur more frequently in later years (a decreased return period) and thus is more likely to occur on any given day when compared to earlier years (Figures 8a and 8b). This increase in occurrence frequency is a combined effect from urbanization and the densification taking place in study areas, irrigation, and changes in *P*. Notably, there is an increase in the short return period events where more *R* occurs with the same return period at the later years (Figures 8c and 8d). The increase is similar between the two sites in earlier years before the irrigation starts to play a role in surface runoff (before 1960s) even though the urbanization scenarios are substantially different. The effect of irrigation restrictions starting from 1992 is seen as a clear decrease in the amount of daily runoff (Figures 8c and 8d). This decrease is more visible in Oakridge neighborhood due to substantially larger input of water due to irrigation. The increasing temporal trend of *R* with specific return period decreases when the return period increases (Figures 8c and 8d), and according to Mann-Kendall trend test (Kendall, 1975; Mann, 1945) performed for each year, the variation in runoff events with long return periods (>52 days) has insignificant trend (significance level $\alpha = 0.05$) as the variation is purely caused by different climate conditions between the years. Also, previous studies have found urbanization to affect mainly the events with short return period and not the long return period as during intense precipitation events, the infiltration capacity of pervious surfaces due to soil saturation is exceeded, and thus, the surfaces already start to act as an impervious surfaces (e.g., Braud et al., 2013; Hollis, 1975). As the daily runoff events with high probability (small runoff events) have especially increased, the annual runoff amounts have increased substantially as majority of the daily runoff events using base run are rather small: daily mean values vary annually from 2.96 to 9.76 mm/day in Oakridge neighborhood and 3.23 to 7.76 mm/day in Sunset neighborhood. The low temporal resolution of WATCH precipitation data (3 hr) might cause smaller daily runoffs due to the lack of high intense convective precipitation events that produce high amount of surface runoff. However, with higher resolution precipitation data, the largest impacts are seen on days with greatest daily rainfall (Ward et al., 2017).

3.4. The Impact of Different Irrigation Scenarios

As garden irrigation is a major component of the sites' hydrological cycle, its effect is evaluated in more detail. The portion of annual *R* due to irrigation is calculated as a difference of annual *R* from run in question compared to *no irrigation* run and divided with total annual *R* of that run. In the *no restrictions* run, portion is the highest in 2008: 0.74 and 0.40 in Oakridge and Sunset neighborhoods, respectively. With realistic irrigation in the base run, the portion of annual *R* caused by the irrigation is the highest in 1985 (0.57) in Oakridge

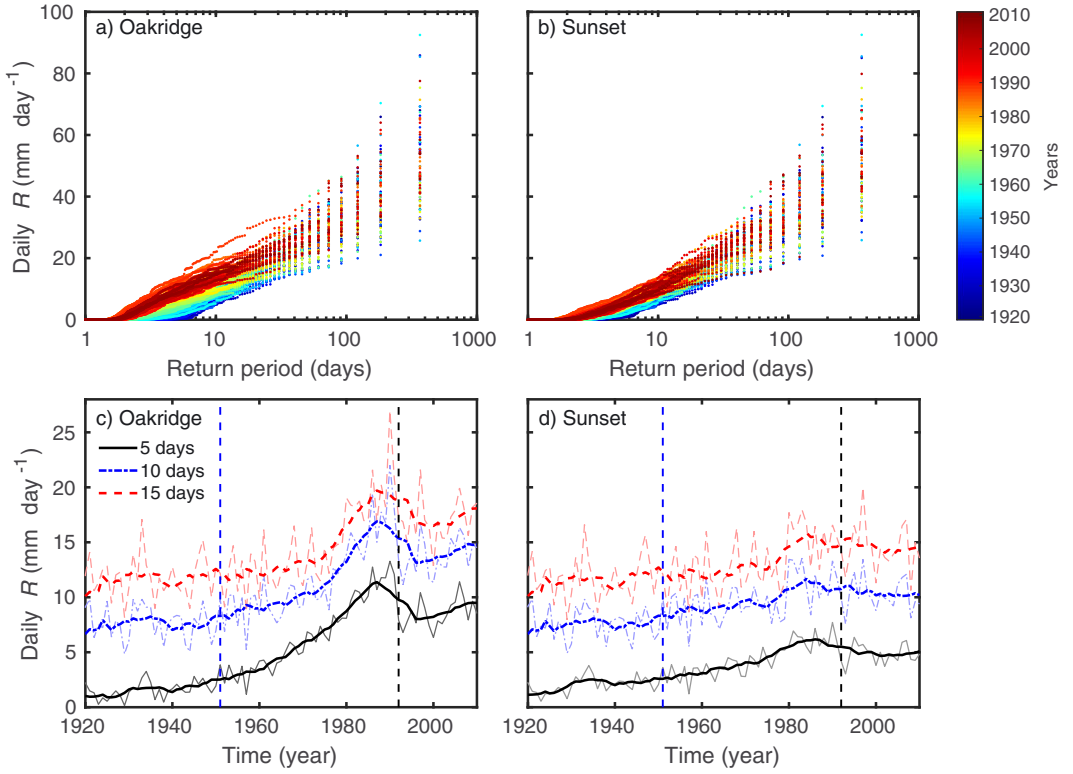

Figure 8. Return periods of daily runoff (R) events for (a) Oakridge and (b) Sunset neighborhoods for each year of the study period (1920–2010) using the base run with the most realistic model parameters. See section 2.5 for method explanation. Annual (lighter curves) and 10-year running mean (bold curves) of surface runoff (R) with different return periods of 5, 10, and 15 days for (c) Oakridge and (d) Sunset neighborhoods using the base run. Start of the irrigation period (1951, blue vertical-dashed line) and start of irrigation restrictions (1992, black vertical-dashed line).

and 1990 (0.29) in Sunset. With the stage 1 restrictions (see Table 2), the highest runoff contributions are in 2008: 0.43 and 0.9, and with stage 2 restrictions in 2008: 0.23 and 0.2, in Oakridge and Sunset neighborhoods, respectively.

The constant surface model run (Table 3) enables us to examine the effect of irrigation (depending also on the climate) on R and E (Figure 9). The R increases linearly with I_e, and when the amount of irrigation is doubled, the amount of runoff increases by 38% in Oakridge neighborhood and 37% in Sunset neighborhood (Figure 9a).

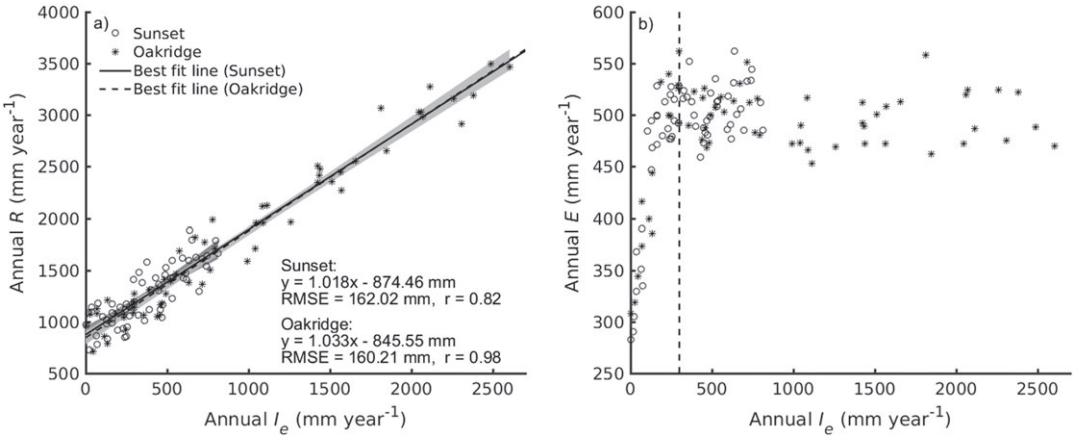

Figure 9. Annual (a) runoff (R) and (b) evaporation (E) as a function of irrigation (I_e) using the constant surface run (Table 3). The gray areas are nonsimultaneous functional bounds with 95% confidence level. The vertical-dashed line is the 300-mm threshold after which the excess water will go to R and not to E. See section 2.5 for statistics explanation.

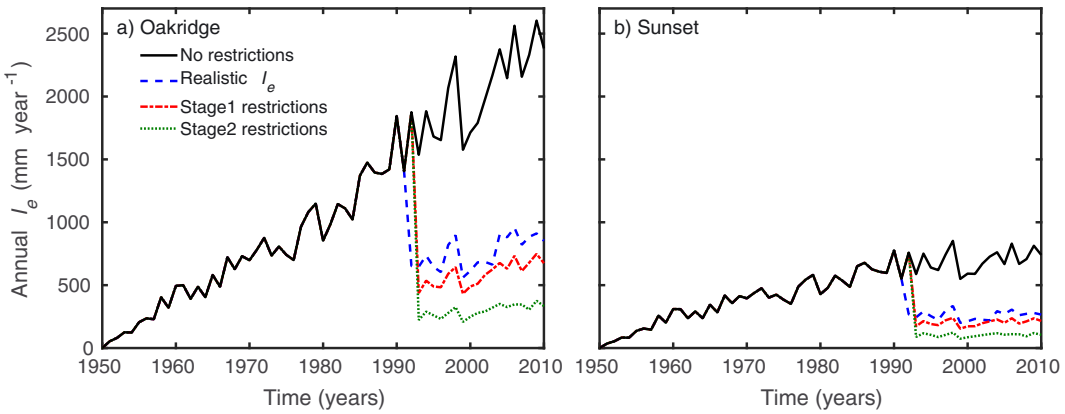

Figure 10. Annual irrigation (I_e) at (a) Oakridge and (b) Sunset neighborhoods with different irrigation scenarios (see Table 2) for the period of irrigation (1951–2010).

Whereas the E dependence on I_e has a very different behavior, the annual E increases rapidly with small I_e, but at 300 mm/year, a threshold is reached after which the annual E stays approximately the same (Figure 9b). The threshold indicates that energy limitations have been met, and excess irrigation is not usable by the garden and its plants, so the additional water goes to the drainage system. Similar thresholds for lawn evaporation have been found and used to determine the required amount of irrigation in other studies (e.g., Danielson et al., 1980).

The threshold value is in line with the lawn irrigation recommendations for the Greater Vancouver area of a 20 mm/week (Metro Vancouver, 2017; once per week for 1 hr, maximum), which adds up to approximately 350 mm during the whole irrigation period (1 May to 31 August). The amount of irrigation applied at study sites however substantially exceeds reasonable garden irrigation even with restrictions applied,

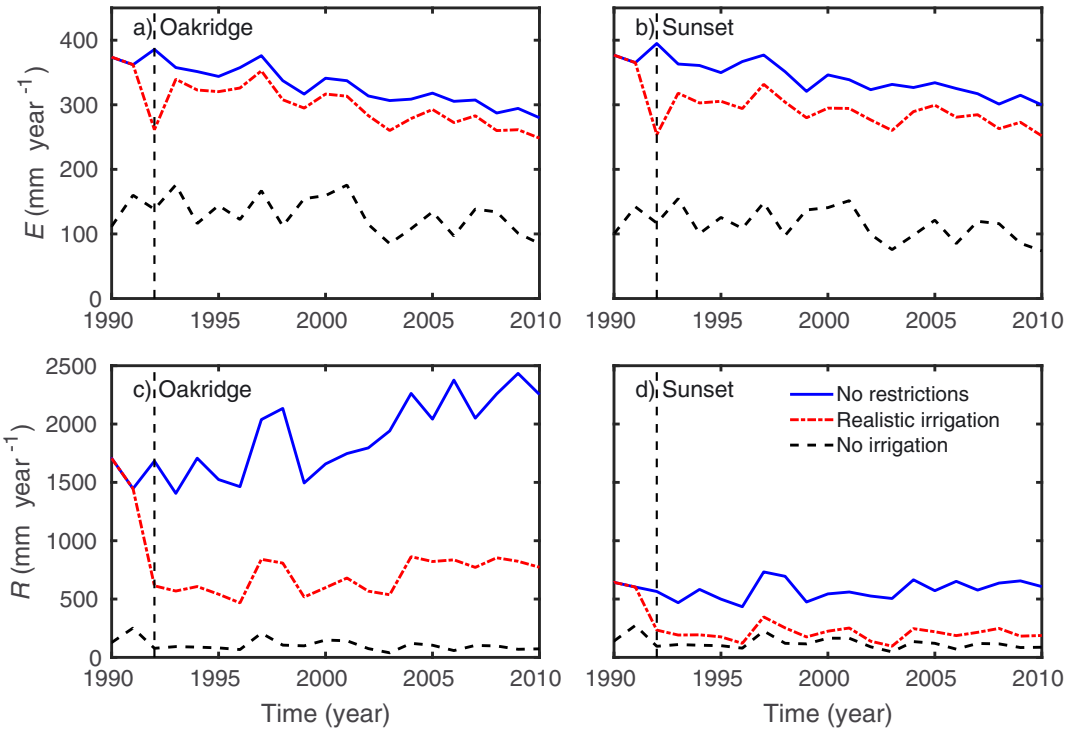

Figure 11. Evaporation (E; a, b) and runoff (R; c, d) totals for the irrigation period (1 May to 31 August) for Oakridge (a, c) and Sunset (b, d) neighborhoods in 1990–2010 with the different irrigation scenarios: no restrictions, realistic irrigation in the base run with restrictions, and no irrigation. Vertical-dashed line shows the start of irrigation restrictions (1992) in the realistic irrigation scenario.

especially in the Oakridge area. For the no restrictions model run, the annual irrigation is the highest in 2009 (2,603 mm/year) in the Oakridge neighborhood and 1998 (852 mm/year) in the Sunset neighborhood (Figure 10). With realistic irrigation (base run), before the restrictions were applied, the annual irrigations are the highest in 1990 (1,845 and 777 mm/year in Oakridge and Sunset, respectively), and when the irrigation restrictions are applied, irrigation is the highest in 2006 (956 mm/year) in Oakridge and 1998 (334 mm/year) in Sunset. With stage 1 restrictions applied throughout the irrigation period (irrigation allowed twice per week; Table 2), irrigation would be the greatest in 2009 (749 mm/year) and 1998 (240 mm/year) and with stage 2 restrictions (irrigation allowed once per week) in 2009 (375 mm/year) and 1998 (123 mm/year) in Oakridge and Sunset neighborhoods, respectively. The average amount of water saved by the irrigation restrictions imposed in Vancouver during period 1992–2010 was 290,000 m^3/year in Oakridge and 65,000 m^3/year in Sunset. The irrigation restrictions are important control mechanism in Vancouver, as residents do not pay based on consumption but a fixed amount. Therefore, irrigation is not discouraged based on water pricing. Although the water use restrictions are imposed to prevent the reservoir levels being depleted too quickly, they are designed to keep the gardens healthy without excessive irrigation. These results imply that if stage 2 restrictions were applied throughout the year, the irrigation would stay near the threshold and the recommended amount of irrigation (Metro Vancouver, 2017) and still permit healthy gardens.

As the threshold in annual E is easily reached at the sites, the imposed irrigation restrictions in the base run do not have big influence on the evaporation during the irrigation period (decreased by 5–15% in Oakridge neighborhood and 10–22% in Sunset neighborhood) except for the 10-week total ban in 1992 that has a clear effect (decreased by 32% in Oakridge and 36% in Sunset; Figure 11). However, the irrigation restrictions have a significant effect on the runoff during the irrigation period decreasing it by 59–72% and 53–81% in Oakridge and Sunset, respectively.

4. Conclusions

In this study we have mapped for the first time in detail the most important factors affecting suburban water balance over a long period via determining the relative contributions of the impacts of land cover changes and irrigation. The long-term hydrological changes of two suburban neighborhoods in Vancouver, BC, are evaluated using SUEWS with WATCH forcing data which has been shown to give reasonable results compared to eddy covariance measurements at the studied sites. The whole lifespan of the areas is examined from prior to urbanization (1920) to when the two areas are dense inner city suburban areas (2010). In order to study the effect of urbanization and subsequent densification on local hydrological cycle in detail, high resolution surface characteristics are determined.

Over the 91 years, garden irrigation has the dominant impact on the suburban hydrological cycle over urbanization and densification accounting for up to 56% of the water input annually and up to 89% during the irrigation period (May–August). Annually surface runoff is linearly dependent on the amount of irrigation at the studied sites: when irrigation is doubled, the runoff increases 38% in Oakridge neighborhood and 37% in Sunset neighborhood. Evaporation on the other hand increases to a threshold value of 300 mm/year which after it is energy limited and excess water is going to runoff. This threshold value is similar to the irrigation recommendations for the Metro Vancouver area. During the past decades, excess irrigation has taken place despite the irrigation restrictions (typically limited to 2 days/week) in Vancouver since 1992, notably in the more prosperous Oakridge area. The average amount of water saved by the irrigation restrictions was approximately 290,000 and 65,000 m^3/year (1,280 and 440 mm/year) in Oakridge and Sunset neighborhoods, respectively. Past restrictions have had only a small effect on annual evaporation as the irrigation amounts have been above the threshold, and stricter restrictions (once per week) would still allow enough irrigation for the lawns to stay healthy while preventing excessive water use.

Land cover changes have also had a substantial effect on the local water and energy balances. Without irrigation, evaporation would have had decreasing trend of 1.3 and 1.4 mm/year and runoff increasing trend of 3.9 and 4.0 mm/year in Oakridge and Sunset neighborhoods, respectively. This is mainly caused by the changes in the land cover despite climate changes causing annual precipitation increase of 2.4 mm/year over the study period. Similarly, the ratio of sensible heat flux over net all-wave radiation plus anthropogenic heat would have had an increasing trend of 0.002 and 0.003 per year over the 91 years. Furthermore, urbanization and densification have substantially increased the runoff coefficients (average increase of 0.14) which increases the risk of surface flooding. In general, the small daily surface runoff events with high probability (short return

period) have increased over the study period, whereas according to trend tests performed, the heavy daily runoff events (return period > 52 days) are not affected.

These results can inform water sensitive urban design and the impacts of the long-term changes on annual hydrological exchanges and return periods. The methodology to assess the amounts of water that can be used by gardens can be applied in regions where irrigation restrictions are planned. The methods presented can be applied to urban hydrological conditions globally, but the model performance and suitability of WATCH forcing data in the focus area should be evaluated. It is crucial that appropriate model parameters are used when applied in substantially different climate conditions from Vancouver.

Acknowledgments
We thank Maj and Tor Nessling Foundation for funding (grant 201400502, 201500273, and 201600458) and Maa- ja vesitekniikan tuki ry (grant 36663). We also thank the Academy of Finland (ICOS-Finland 281255), the Academy of Finland Centre of Excellence (grant 307331), NERC/Belmont TRUC (NE/L008971/1 and G8MUREFU3FP-2201-075), and Newton Fund/Met Office CSSP-China (Grimmond). Data collection at Sunset neighborhood was financially supported by the Canadian Foundation for Climate and Atmospheric Sciences (CFCAS) as part of the Network "Environmental Prediction in Canadian Cities" (EPiCC), by NSERC (RGPIN 342029-12), and the Canadian Foundation for Innovation (CFI) (grant 17141 and 33600). We acknowledge the City of Vancouver for providing historical photographs, maps, and assessment data of the study areas. The data used are listed in the references, tables, and supplements. For SUEWS manual and software, visit http://suews-docs.readthedocs.io.

References

Alexander, P. J., Bechtel, B., Chow, W. T. L., Fealy, R., & Mills, G. (2016). Linking urban climate classification with an urban energy and water budget model: Multi-site and multi-seasonal evaluation. *Urban Climate*, *17*, 196–215. https://doi.org/10.1016/j.uclim.2016.08.003

Alexander, P. J., Mills, G., & Fealy, R. (2015). Using LCZ data to run an urban energy balance model. *Urban Climate*, *13*, 14–37. https://doi.org/10.1016/j.uclim.2015.05.001

Barron, O. V., Barr, A. D., & Donn, M. J. (2013). Effect of urbanization on the water balance of a catchment with shallow groundwater. *Journal of Hydrology*, *485*, 162–176. https://doi.org/10.1016/j.jhydrol.2012.04.027

Best, M. J., & Grimmond, C. S. B. (2016). Modelling the partitioning of turbulent fluxes at urban sites with varying vegetation cover. *Journal of Hydrometeorology*, *17*, 2537–2553. https://doi.org/10.1175/JHM-D-15-0126.1

Boyd, M. J., Bufill, M. C., & Knee, R. M. (1993). Pervious and impervious runoff in urban catchments. *Hydrological Sciences Journal*, *38*(6), 463–478. https://doi.org/10.1080/02626669309492699

Braud, I., Breil, P., Thollet, F., Lagouy, M., Branger, F., Jacqueminet, C., et al. (2013). Evidence of the impact of urbanization on the hydrological regime of a medium-sized periurban catchment in France. *Journal of Hydrology*, *485*, 5–23. https://doi.org/10.1016/j.jhydrol.2012.04.049

Burton, G. A., & Pitt, R. (2002). *Stormwater effects handbook: A toolbox for watershed managers, scientists, and engineers*. Boca Raton, FL: CRC Press.

Canada Statistics (1988). Census tracts, Vancouver: Part 2, profiles, 1986 Census of Canada. Catalogue, 95-168.

Christen, A., Crawford, B., & Oke, T. (2009). Water metering in the Vancouver EPiCC neighborhoods (EPiCC Technical Report No. 5). Department of Geography, University of British Columbia.

City of Vancouver (2015). VanMap, orthophotos for 2009 and 1999, (accessed, June 2015).

Cleugh, H. A., & Oke, T. R. (1986). Suburban-rural energy balance comparisons in summer for Vancouver, B.C. *Boundary-Layer Meteorology*, *36*(4), 351–369. https://doi.org/10.1007/BF00118337

Crawford, B., Christen, A., & Ketler, R. (2010). Processing and quality control procedures of turbulent flux measurements during the Vancouver EPiCC experiment (EPiCC Technical Report No, 1). Department of Geography, University of British Columbia. https://doi.org/10.14288/1.0103593

Dams, J., Dujardin, J., Reggers, R., Bashir, I., Canters, F., & Batelaan, O. (2013). Mapping impervious surface change from remote sensing for hydrological modeling. *Journal of Hydrology*, *485*, 84–95. https://doi.org/10.1016/j.jhydrol.2012.09.045

Danielson, R. E., Hart, W. E., Feldhake, C. M., & Haw, P. M. (1980). Water requirements for urban lawns in Colorado (Completion report No. 97). Colorado State University.

Dee, D. P., Uppala, S. M., Simmons, A. J., Berrisford, P., Poli, P., Kobayashi, S., et al. (2011). The ERA-Interim reanalysis: Configuration and performance of the data assimilation system. *Quarterly Journal of the Royal Meteorological Society*, *137*, 553–597. https://doi.org/10.1002/qj.828

Demuzere, M., Coutts, A. M., Göhler, M., Broadbent, A. M., Wouters, H., van Lipzig, N. P. M., & Gebert, L. (2014). The implementation of biofiltration systems, rainwater tanks and urban irrigation in a single-layer urban canopy model. *Urban Climate*, *10*(part 1), 148–170. https://doi.org/10.1016/j.uclim.2014.10.012

Demuzere, M., Harshan, S., Järvi, L., Roth, M., Grimmond, C. S. B., Masson, V., et al. (2017). Impact of urban canopy models and external parameters on the modelled urban energy balance in a tropical city. *Quarterly Journal of the Royal Meteorological Society*, *143*(704), 1581–1596. https://doi.org/10.1002/qj.3028

Dominion Bureau of Statistics (1953). Population and housing characteristics by census tracts, Vancouver, 1951 Census of Canada. Bulletin CT-11, Ottawa.

Dominion Bureau of Statistics (1957). Population characteristics by census tracts, Vancouver, 1956 Census of Canada. Bulletin, 4-14.

Dominion Bureau of Statistics (1968). Population characteristics by census tracts, Vancouver, 1966 Census of Canada. Catalogue 95-627 (C-27).

Egeinbrod, F., Bell, V. A., Davies, H. N., Heinemeyer, A., Armsworth, P. R., & Gaston, K. J. (2011). The impact of projected increases in urbanization on ecosystem services. *Proceedings of the Royal Society: B*, *278*, 3201–3208. https://doi.org/10.1098/rspb.2010.2754

Falk, J., & Niemczynowicz, J. (1979). Characteristics of the above ground runoff in sewered catchments. In P. R. Helliwell (Ed.), *Urban storm drainage* (pp. 159–171). London: Pentech.

Fletcher, T. D., Andrieu, H., & Hamel, P. (2013). Understanding, management and modelling of urban hydrology and its consequences for receiving waters: A state of the art review. *Advances in Water Resources*, *51*, 261–279. https://doi.org/10.1016/j.advwatres.2012.09.001

Geographic Information Centre (2015). Aerial photographs from the University Air Photo Collection.

Gober, P., Brazel, A., Quay, R., Myint, S., Grossman-Clarke, S., Miller, A., & Rossi, S. (2009). Using watered landscapes to manipulate urban heat island effects: How much water will it take to cool Phoenix? *Journal of the American Planning Association*, *76*(1), 109–121. https://doi.org/10.1080/01944360903433113

Gober, P., Kirkwood, C. W., Balling, R. C. Jr., Ellis, A. W., & Deitrick, S. (2010). Water planning under climatic uncertainty in Phoenix: Why we need a new paradigm. *Annals of the Association of American Geographers*, *100*(2), 356–372. https://doi.org/10.1080/00045601003595420

Goldshleger, N., Shoshany, M., Kandibad, L., Arbel, S., & Getker, M. (2009). Generalising relationships between runoff-rainfall coefficients and impervious areas: An integration of data from case studies in Israel with data sets from Australia and the USA. *Urban Water Journal*, *6*(3), 201–208. https://doi.org/10.1080/15730620802246355

Grimmond, C. S. B. (1992). The suburban energy balance: Methodological considerations and results for a mid-latitude west coast city under winter and spring conditions. *International Journal of Climatology*, *12*(5), 481–497. https://doi.org/10.1002/joc.3370120506

Grimmond, C. S. B., & Oke, T. R. (1986a). Urban water balance: 2. Results from a suburb of Vancouver, British Columbia. *Water Resources Research*, *22*(10), 1404–1412. https://doi.org/10.1029/WR022i010p01404
Grimmond, C. S. B., & Oke, T. R. (1986b). Urban water balance: 1. A model for daily totals. *Water Resources Research*, *22*(10), 1397–1403. https://doi.org/10.1029/WR022i010p01397
Grimmond, C. S. B., & Oke, T. R. (1991). An evapotranspiration-interception model for urban areas. *Water Resources Research*, *27*(7), 1739–1755. https://doi.org/10.1029/91WR00557
Grimmond, C. S. B., & Oke, T. R. (1999a). Evapotranspiration rates in urban areas. In J. B. Ellis (Ed.), *Impacts of urban growth on surface water and groundwater quality* (Vol. 259, pp. 235–243). Wallingford, UK: International Association of Hydrological Sciences.
Grimmond, C. S. B., & Oke, T. R. (1999b). Aerodynamic properties of urban areas derived from analysis of surface form. *Journal of Applied Meteorology*, *38*, 1262–1292. https://doi.org/10.1175/1520-0450(1999)038<1262:APOUAD>2.0.CO;2
Hall, K. J., & Schreier, H. (1996). Urbanization and agricultural intensification in the Lower Frases River Valley: Impacts on water use and quality. *GeoJournal*, *40*(1), 135–146. https://doi.org/10.1007/BF00222539
Hare, F. K., & Thomas, M. K. (1979). *Climate Canada* (2nd ed.). Canada: John Wiley & Sons.
Hillel, D. (1971). *Soil and water: Physical principles and processes*. New York: Academic Press.
Hirsch, R. M., Slack, J. R., & Smith, R. A. (1982). Tecniques of trend analysis for monthly water quality data. *Water Resources Research*, *18*(1), 107–121. https://doi.org/10.1029/WR018i001p00107
Hollis, G. (1975). The effect of urbanization on floods of different recurrence interval. *Water Resources Research*, *11*(3), 431–435. https://doi.org/10.1029/WR011i003p00431
House-Peters, L. A., & Chang, H. (2011). Urban water demand modeling: Review of concepts, methods, and organizing principles. *Water Resources Research*, *47*, W05401. https://doi.org/10.1029/2010WR009624
Järvi, L., Grimmond, S., & Christen, A. (2011). The Surface Urban Energy and Water Balance Scheme (SUEWS): Evaluation in Los Angeles and Vancouver. *Journal of Hydrology*, *411*, 219–237. https://doi.org/10.1016/j.jhydrol.2011.10.001
Järvi, L., Grimmond, C. S. B., McFadden, J. P., Christen, A., Strachan, I. B., Taka, M., et al. (2017). Warming effects on the urban hydrology in cold climate regions. *Scientific Reports*, *7*, 5833. https://doi.org/10.1038/s41598-017-05733-y
Järvi, L., Grimmond, C. S. B., Taka, M., Nordbo, A., Setälä, H., & Strachan, I. B. (2014). Development of the Surface Urban Energy and Water Balance Scheme (SUEWS) for cold climate cities. *Geoscientific Model Development*, *7*, 1691–1711. https://doi.org/10.5194/gmd-7-1691-2014
Kalanda, B. D., Oke, T. R., & Spittlehouse, D. L. (1980). Suburban energy balance estimates for Vancouver, B.C., using the Bowen ratio-energy balance approach. *Journal of Applied Meteorology*, *19*, 791–802. https://doi.org/10.1175/1520-0450(1980)019<0791:SEBEFV>2.0.CO;2
Karsisto, P., Fortelius, C., Demuzere, M., Grimmond, C. S. B., Oleson, K. W., Kouznetsov, R., et al. (2016). Seasonal surface urban energy balance and wintertime stability simulated using three land-surface models in the high-latitude city Helsinki. *Quarterly Journal of the Royal Meteorological Society*, *142*(694), 401–417. https://doi.org/10.1002/qj.2659
Kendall, M. G. (1975). *Rank correlation methods*. London: Charles Griffin.
Kennedy, D. S., Klein, R. A., & Clark, M. P. (2004). Use and effectiveness of municipal water restrictions during drought in Colorado. *Journal of the American Water Resources Association*, *40*(1), 77–87. https://doi.org/10.1111/j.1752-1688.2004.tb01011.x
Kokkonen, T. V., Grimmond, C. S. B., Räty, O., Ward, H. C., Christen, A., Oke, T. R., et al. (2018). Sensitivity of Surface Urban Energy and Water Balance Scheme (SUEWS) to downscaling of reanalysis forcing data. *Urban Climate*, *23*, 36–52. https://doi.org/10.1016/j.uclim.2017.05.001
Leopold, L. B. (1968). Hydrology for urban land planning—A guidebook on the hydrologic effect of urban land use. U.S. Geological survey Circular nr 554, U.S. department of the interior.
Lins, H. F., & Slack, J. R. (1999). Streamflow trends in the United States. *Geophysical Research Letters*, *26*(2), 227–230. https://doi.org/10.1029/1998GL900291
Liss, K., Tooke, R., Heyman, E., Coops, N., & Christen, A. (2010). Vegetation characteristics at the Vancouver EPiCC experimental sites (EPiCC Technical Report No. 3). University of British Columbia. https://doi.org/10.14288/1.0103589, Technical Report of the Department of Geography.
Mann, H. B. (1945). Nonparametric tests against trend. *Econometrica*, *13*(3), 245–259.
McPherson, E. G., van Doorn, N. S., & Peper, P. J. (2016a). Urban tree database and allometric equations (General technical report PSW-GTR-253). Albany, CA: U.S. Department of Agriculture, Forest Service.
McPherson, E. G., van Doorn, N. S., & Peper, P. J. (2016b). Urban tree database. https://doi.org/10.2737/RDS-2016-0005
Metro Vancouver (2010). Don't waste water on your lawn, Media release May 31, 2010.
Metro Vancouver (2011). 2010 Water Consumption Statistics Report, Operations and Mainteinance Department.
Metro Vancouver (2017). Waterwise lawn care brochure, accessed 10 April 2017.
Ministry of Environment (2016). Indicators of climate change for British Columbia, 2016 update.
Mitchell, V. G., McMahon, T. A., & Mein, R. G. (2003). Components of the total water balance of an urban catchment. *Environmental Management*, *32*(6), 735–746. https://doi.org/10.1007/s00267-003-2062-2
Mitchell, V. G., Mein, R. G., & McMahon, T. A. (2001). Modelling the urban water cycle. *Environmental Modelling and Software*, *16*, 615–629. https://doi.org/10.1016/S1364-8152(01)00029-9
Monteith, J. L. (1965). Evaporation and the environment. *Symposia of the Society for Experimental Biology*, *19*, 205–234.
Oke, T. R. (1979). Advectively-assisted evapotranspiration from irrigated urban vegetation. *Boundary-Layer Meteorology*, *17*(2), 167–173. https://doi.org/10.1007/BF00117976
Oke, T. R., Cleugh, H. A., Grimmond, S., Schmid, H. P., & Roth, M. (1989). Evaluation of spatially-averaged fluxes of heat, mass and momentum in the urban bounday layer. *Weather and Climate*, *9*, 14–21.
Oke, T., & Hay, J. (1994). *The climate of Vancouver* (2nd ed.). no. 50 in B.C. geographical series. University of British Columbia: Department of Geography.
Oke, T. R., & McCaughey, J. H. (1983). Suburban-rural energy balance comparisons for Vancouver, B.C.: An extreme case? *Boundary-Layer Meteorology*, *26*(4), 337–354. https://doi.org/10.1007/BF00119532
Oke, T. R., Mills, G., Christen, A., & Voogt, J. A. (2017). *Urban climates*. Cambridge, UK: Cambridge University Press. https://doi.org/10.1017/9781139016476
Pauleit, S., Ennos, R., & Golding, Y. (2005). Modeling the environmental impacts of urban land use and land cover change—A study in Merseyside, UK. *Landscape and Urban Planning*, *71*, 295–310. https://doi.org/10.1016/j.landurbplan.2004.03.009
Pechlivanidis, I. G., Arheimer, B., Donnelly, C., Hundecha, Y., Huang, S., Aich, V., et al. (2017). Analysis of hydrological extremes at different hydro-climatic regimes under present and future condition. *Climatic Change*, *141*(3), 467–481. https://doi.org/10.1007/s10584-016-1723-0

Penman, H. L. (1948). Natural evaporation from open water, bare soil and grass. *Home Proceedings of the Royal Society of London A: Mathematical*, *193*(1032), 120–145. https://doi.org/10.1098/rspa.1948.0037
Rain Bird Corporation (2016). Rain Bird virtual museum: Decades of innovation. accessed September 2016.
Ramamurthy, P., & Bou-Zeid, E. (2014). Contribution of impervious surface to urban evaporation. *Water Resources Research*, *50*, 2889–2902. https://doi.org/10.1002/2013WR013909
Rodriguez, F., Andrieu, H., & Creutin, J.-D. (2003). Surface runoff in urban catchment: Morphological identification of unit hydrographs from urban databanks. *Journal of Hydrology*, *283*, 146–168. https://doi.org/10.1016/S0022-1694(03)00246-4
Sailor, D. J. (2011). A review of methods for estimating anthropogenic heat and moisture emissions in the urban environment. *International Journal of Climatology*, *31*, 189–199. https://doi.org/10.1002/joc.2106
Schmid, H. P., Cleugh, H. A., Grimmond, C. S. B., & Oke, T. R. (1991). Spatial variability of energy fluxes in suburban terrain. *Boundary-Layer Meteorology*, *54*(3), 249–276. https://doi.org/10.1007/BF00183956
Schneider, U., Becker, A., Finger, P., Meyer-Christoffer, A., Ziese, M., & Rudolf, B. (2013). GPCC's new land surface precipitation climatology based on quality-controlled in situ data and its role in quantifying the global water cycle. *Theoretical and Applied Climatology*, *115*, 15–40. https://doi.org/10.1007/s00704-013-0860-x
Shuster, W. D., Bonta, J., Thurston, H., Warnemuende, E., & Smith, D. R. (2005). Impacts of impervious surface on watershed hydrology: A review. *Urban Water Journal*, *2*(4), 263–275. https://doi.org/10.1080/15730620500386529
Shuttleworth, W. J. (1978). A simplified one-dimensional theoretical description of the vegetation-atmosphere interaction. *Boundary-Layer Meteorology*, *14*(1), 3–27. https://doi.org/10.1007/BF00123986
Statistics Canada (1974). Population and charasteristics by census tracts, Vancouver, 1971 Census of Canada. Catalogue 95-758 (CT28B).
Statistics Canada (1978). Census tracts, population and housing charasteristics, Vancouver, 1976 census of Canada. Catalogue 95-828 (bulletin 6.29).
Statistics Canada (1984). 1981 Census of Canada. Tech. rep.
Statistics Canada (1999). Population and dwelling counts, for enumeration areas, 1996 Census - 100 % data. Catalogue 93F0032XDB96022.
Statistics Canada (2002). Population and dwelling counts, 2001 census. Catalogue 93F0051XIE.
Statistics Canada (2007). Population and dwelling counts, 2006 census, 100 % data. Catalogue 97-550-XWE2006002.
Statistics Canada (2012). GeoSearch, 2011 census, Statistics Canada catalogue no. 92-142-xwe.
Stewart, I. D., & Oke, T. R. (2012). Local climate zones for urban temperature studies. *Bulletin of the American Meteorological Society*, *93*(12), 1879–1900. https://doi.org/10.1175/BAMS-D-11-00019.1
Tokarczyk, P., Leitao, J. P., Rieckermann, J., Schindler, K., & Blumensaat, F. (2015). High-quality observation of surface imperviousness for urban runoff modelling using UAV imagery. *Hydrology and Earth System Sciences*, *19*, 4215–4228. https://doi.org/10.5194/hess-19-4215-2015
Uppala, S. M., Kållberg, P. W., Simmons, A. J., Andrae, U., Da Costa Bechtold, V., Fiorino, M., et al. (2005). The ERA-40 re-analysis. *Quarterly Journal of the Royal Meteorological Society*, *131*(612), 2961–3012. https://doi.org/10.1256/qj.04.176
van der Laan, M., Tooke, R., Christen, A., Coops, N., Heyman, E., & Olchovski, I. (2012). Statistics on the built infrastructure at the Vancouver EPiCC experimental sites (EPiCC Technical Report No. 4). https://doi.org/10.14288/1.0103592, technical Report of the Department of Geography.
Vancouver (BC), Planning department (1963). City of Vancouver, households and population by enumeration areas, 1961 Census of Canada. Cartographic material COV-S445-3-: MAP.
Velpuri, N. M., & Senay, G. B. (2013). Analysis of long-term trends (1950–2009) in precipitation, runoff and runoff coefficient in major urban watersheds in the United States. *Environmental Research Letters*, *8*(2), 1–6. https://doi.org/10.1088/1748-9326/8/2/024020
Ward, H., & Grimmond, C. (2017). Assessing the impact of changes in surface cover, human behaviour and climate on energy partitioning across Greater London. *Landscape and Urban Planning*, *165*, 142–161. https://doi.org/10.1016/j.landurbplan.2017.04.001
Ward, H. C., Järvi, L., Onomura, S., Lindberg, F., Gabey, A., & Grimmond, C. S. B. (2016). SUEWS Manual V2016a.
Ward, H. C., Kotthaus, S., Järvi, L., & Grimmond, C. S. B. (2016). Surface Urban Energy and Water Balance Scheme (SUEWS): Development and evaluation at two UK sites. *Urban Climate*, *18*, 1–32. https://doi.org/10.1016/j.uclim.2016.05.001
Ward, H. C., Tan, Y. S., Gabey, A. M., Kotthaus, S., & Grimmond, C. S. B. (2017). Impact of temporal resolution of precipitation forcing data on modelled urban-atmosphere exchanges and surface conditions. *International Journal of Climatology*, *38*(2), 649–662. https://doi.org/10.1002/joc.5200
Weedon, G. P., Balsamo, G., Bellouin, N., Gomes, S., Best, M., & Viterbo, P. (2014). The WFDEI meteorological forcing data set: WATCH Forcing Data methodology applied to ERA-Interim reanalysis data. *Water Resources Research*, *50*, 7505–7514. https://doi.org/10.1002/2014WR015638
Weedon, G. P., Gomes, S., Viterbo, P., Österle, H., Adam, J. C., Bellouin, N., et al. (2010). The WATCH Forcing Data 1958–2001: A meteorological forcing dataset for land surface- and hydrological models. WATCH Technical Report, 22.
Weedon, G. P., Gomes, S., Viterbo, P., Shuttleworth, W. J., Blyth, E., Österle, H., et al. (2011). Creation of WATCH Forcing Data and its use to assess global and regional reference crop evaporation over land during the twentieth century. *Journal of Hydrometeorology*, *12*, 823–848. https://doi.org/10.1175/2011JHM1369.1
Weibull, W. (1939). A statistical theory of the strength of materials. *Ingeniörsvetenskapsakademiens Handlingar*, *151*, 1–45.
White, M. D., & Greer, K. A. (2006). The effects of watershed urbanization on the stream hydrology and reparian vegetation of Los Peñasquitos Creek, California. *Landscape and Urban Planning*, *74*(2), 125–138. https://doi.org/10.1016/j.landurbplan.2004.11.015
World Meteorological Organization (2011). *Guide to climatological practices*, vol. WMO-No, 100. Geneva: World Meteorological Organization.
Zhang, X., Vincent, L. A., Hogg, W. D., & Niitsoo, A. (2000). Temperature and precipitation trends in Canada during the 20th century. *Atmosphere-Ocean*, *38*(3), 395–429. https://doi.org/10.1080/07055900.2000.9649654